

Cross-sectional Imaging of Gallbladder Carcinoma: An Update



Naveen Kalra^{*}, Pankaj Gupta^{*}, Manphool Singhal^{*}, Rajesh Gupta[†], Vikas Gupta[†], Radhika Srinivasan[‡], Bhagwant R. Mittal[§], Radha K. Dhiman[¶], Niranjan Khandelwal^{*}

^{*}Department of Radiodiagnosis and Imaging, Postgraduate Institute of Medical Education and Research (PGIMER), Chandigarh 160012, India, [†]Department of General Surgery, Postgraduate Institute of Medical Education and Research (PGIMER), Chandigarh 160012, India, [‡]Department of Cytology, Postgraduate Institute of Medical Education and Research (PGIMER), Chandigarh 160012, India, [§]Department of Nuclear Medicine, Postgraduate Institute of Medical Education and Research (PGIMER), Chandigarh 160012, India and [¶]Department of Hepatology, Postgraduate Institute of Medical Education and Research (PGIMER), Chandigarh 160012, India

Gallbladder Carcinoma (GBCA) is the most common biliary tract malignancy. As the disease is often diagnosed clinically in an advanced stage, the survival rates are dismal. Imaging studies allow for an early diagnosis of malignancy, though the findings may be indistinguishable from non-malignant disease processes affecting the gallbladder. Attempts have been made to make a specific diagnosis of GBCA at an early stage on imaging studies. Ultrasonography (US) is the most commonly employed technique for gallbladder evaluation. Gallbladder wall thickening is the most common finding of early GBCA and in this context, US is non-specific. Recently, contrast enhanced ultrasound has been shown to be effective in differentiating benign from malignant disease. Multi-detector computed tomography represents the most robust imaging technique in evaluation of GBCA. It provides relatively sensitive evaluation of mural thickening, though it is not entirely specific and issues in differentiating GBCA from xanthogranulomatous cholecystitis do arise. Due to its superior soft tissue resolution, Magnetic Resonance Imaging (MRI) provides excellent delineation of gallbladder and biliary tree involvement. When coupled with functional MRI techniques, such as diffusion-weighted and perfusion imaging, it provides a useful problem solving tool for interrogating the malignant potential of nonspecific gallbladder lesions and detection of metastases. Positron emission tomography has a role in detection of distant metastases and following patients following treatment for malignancy. We review the current role of various imaging modalities in evaluating patients with GBCA. (J CLIN EXP HEPATOL 2019;9:334-344)

Gallbladder Carcinoma (GBCA) is the fifth most common malignancy of the gastrointestinal tract.¹ Recent advances in cross-sectional imaging techniques have increased the preoperative detection rates of GBCA. Nevertheless, an accurate preoperative diagnosis of GBCA is still a daunting task. This is due to the non-specific appearance of early GBCA.² Gallbladder wall thickening is the most common finding of early GBCA.² However, it is also the most common presentation of benign biliary tract disorders. In advanced GBCA, the key issue is the local tumor stage and presence of distant metastasis. This guides the management plan and type and extent of cholecystectomy. Imaging modalities have

shown improved performance over years due to path breaking advances. Notwithstanding, familiarity with appropriate application and interpretation is required to harvest the full potential of various imaging techniques.

Though Ultrasonography (US) is the primary imaging modality in evaluation of biliary tract disorders,³ conventional US is unable to distinguish benign from early malignant disease processes.⁴ Contrast Enhanced Ultrasound (CEUS) is a promising tool but its role in GBCA is not well recognized.⁵ Role of endoscopic ultrasound in GBCA is also limited.⁶ Several studies have validated the sensitivity, specificity and overall accuracy of Multidetector Computed Tomography (MDCT) in pre-operative detection as well as local staging of GBCA.⁷⁻⁹ The sensitivity for detection of nodal and peritoneal metastases is relatively low.⁸ MDCT also allows mapping of vascular anatomy in patients being planned for resection.⁸ Magnetic Resonance Imaging (MRI) provides excellent soft tissue resolution and non-invasive depiction of the biliary tree.⁹ It can be employed as a problem solving tool in situations where evaluation with other imaging modalities is non-conclusive. Recent advances in MRI including Diffusion-Weighted Imaging (DWI) and perfusion imaging may allow a greater accuracy in detection of smaller lesions.⁹⁻¹³ MRI has a greater sensitivity in detection of

Keywords: carcinoma, gallbladder, imaging

Received: 24 August 2017; **Accepted:** 20 April 2018; **Available online:** 30 April 2018

Address for correspondence: Naveen Kalra, Professor, Department of Radiodiagnosis and Imaging, PGIMER, Chandigarh, India. Tel.: +91 9855426320.

E-mail: Navkal2004@yahoo.com

Abbreviations: CEUS: Contrast Enhanced Ultrasound; GBCA: Gallbladder Carcinoma; HRUS: High Resolution US; MDCT: Multidetector Computed Tomography; MRI: Magnetic Resonance Imaging; PET: Positron Emission Tomography; US: Ultrasonography

<https://doi.org/10.1016/j.jceh.2018.04.005>

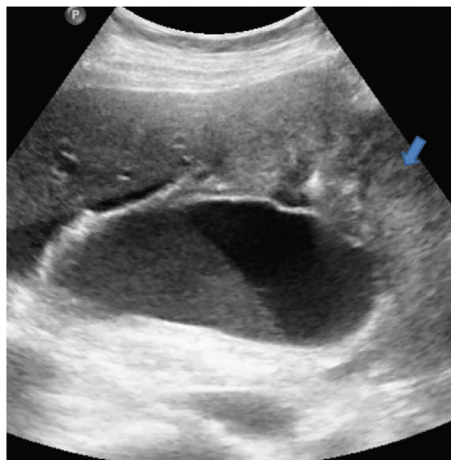


Figure 1 Gray-scale US image shows distended GB showing hyperechoic intraluminal contents forming a level suggestive of sludge. If motionless on changing the patient position, this can potentially mimic an endophytic growth. Also seen in the image is a mass arising from the fundus (arrow).

perihilar lymph nodes and liver metastases.¹² Positron Emission Tomography (PET) is primarily employed in detection of distant metastases and post-treatment detection of residual or recurrent disease.¹⁴

VARIOUS IMAGING TECHNIQUES

Ultrasonography

Conventional US

Conventional US is the first-line modality for the evaluation of GB diseases.³ US has limited utility in differentiation of mural thickening resulting from chronic cholecystitis from that of GBCA.⁴ Sometimes, the biliary sludge is motionless and simulates GBCA on US (Figure 1).⁵ Finally, co-existence of gallbladder inflammation and GBCA is not rare and such cases may be difficult to diagnose with US.⁵ US also fails to provide accurate estimate of local invasion of the GB wall, adjacent liver infiltration (Figure 2), nodal and peritoneal metastases.⁵ GB polyps are common (Figure 3) and malignancy is usually associated with larger polyps. US Doppler has a sensitivity and specificity of around 80% in diagnosis of GBCA. Detection of color flow within a lesion support GBCA (Figure 4), however, its absence does not exclude malignancy. Cut-off value of 20–30 cm/s is proposed for differentiation between benign and malignant disease.

The poor sensitivity has been reported by Bach et al. who found that only 37% cases of advanced disease could be identified on conventional US.¹⁵ Similarly, Tsuchiya reported a high false negative rate of conventional US in early GBCA (Table 1).¹⁶

High Resolution US

Compared to conventional US, High Resolution US (HRUS) has a higher diagnostic accuracy in distinguishing neoplastic polyps and staging GBCA.¹⁷ In a study by Kim et al.

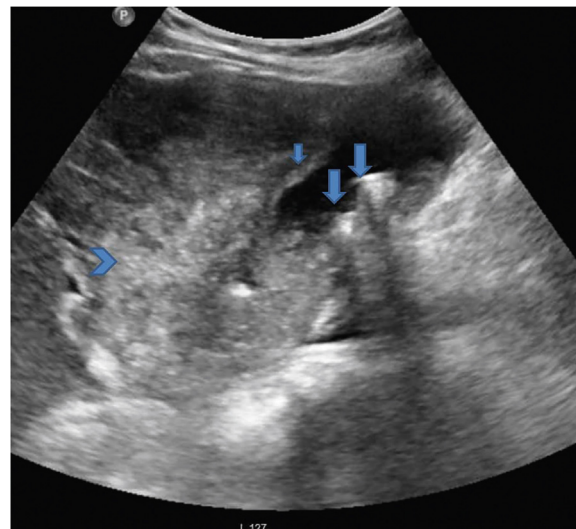


Figure 2 Gray-scale US image shows multiple GB calculi (arrows), GB wall thickening (short arrow) and ill-defined heterogeneous mass arising from the neck of GB (arrow head). CT scores over US in depicting the true extent of adjacent liver invasion.

including 15 malignant polyps and 37 GBCA, sensitivity and specificity for diagnosing malignant polyp were 66.6% and 89.2% respectively.¹⁷ The diagnostic accuracy for T stage was 92–95% for T1a, 89–95% for T1b, 78–86% for T2 and 84–89% for T3 disease. In another study comparing HRUS with Endoscopic Ultrasound (EUS) for staging GBCA, sensitivity, specificity, Positive Predictive Value (PPV) and Negative Predictive Value (NPV) were 82.7%, 44.4%, 82.7% and 44% for HRUS and 86.2%, 22.2%, 78.1% and 33.3% for EUS respectively.¹⁸ For differential diagnosis of GB polyp, sensitivity, specificity, PPV and NPV was 80%, 80%, 86% and 73% using HRUS and 73%, 85%, 88% and 69% using EUS.¹⁸ In a study comparing diagnostic accuracy of HRUS with EUS and CT for polypoidal lesions and GBCA,¹⁹ HRUS had 90% diagnostic accuracy compared to 86% and 72% for EUS and CT. For evaluating the depth of invasion, HRUS had a diagnostic accuracy of 62.9% compared to 55.5% and 44.4% for EUS and CT. Choi et al.²⁰ assessed the HRUS and texture features of risk stratification of GB polyp > 10 mm. A total of 136 patients with GB polyp (>10 mm) underwent both HRUS and cholecystectomy. HRUS features to differentiate carcinoma from adenoma were larger size and sessile nature (93.5–95.7% sensitivity).

CEUS

CEUS has been used successfully in liver, kidney and pancreas.²¹ This and the relative lack of specificity of conventional US has prompted its use in GBCA.²² However, the reports of usefulness of CEUS in GBCA have been conflicting.^{23–38} In one of the earliest works with CEUS, Kato et al.²⁵ found no significant difference between polypoid GBCA and cholesterol polyp in the enhancement pattern and the duration of enhancement. More recent

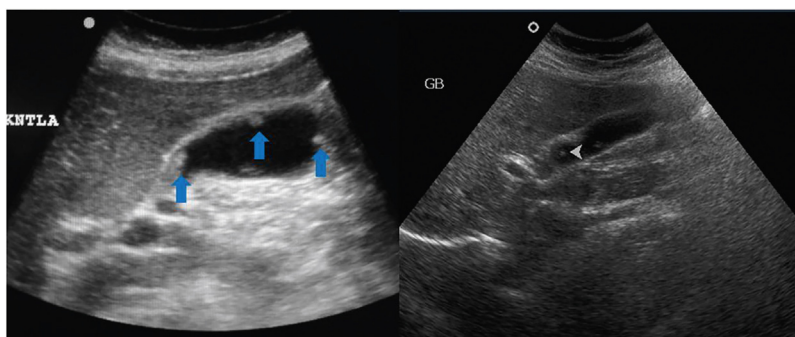


Figure 3 Gray-scale US image shows multiple GB polyps (arrows) in two patients.

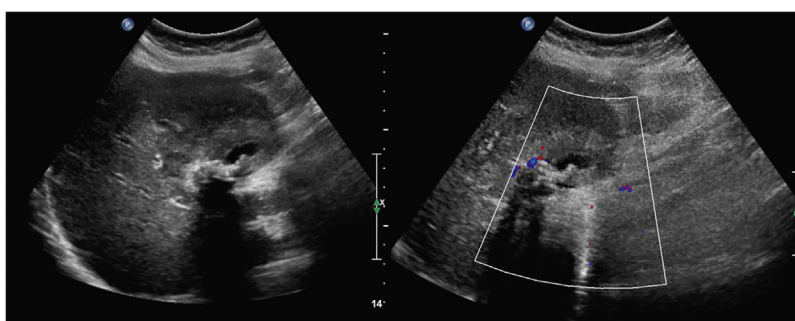


Figure 4 Gray-scale and Doppler US image show GB mass with internal vascularity.

Table 1 Comparison of Diagnostic Performance of Various Imaging Modalities for GBCA.

Feature	Sensitivity	Specificity
Diagnosis of malignancy-GB wall thickening ^{17,18,38,42,57,58}	US: 44%	US: NA
	EUS: 89.6%	EUS: 98%
	CT: 82.5%	CT: 75.9%
	MRI: 100%	MRI: 70%
	FDG-PET: 83.3%	FDG-PET: 89.5%
Diagnosis of malignancy-polyp ^{17,18,58}	HRUS: 66.7%	HRUS: 89.1%
	EUS: 85–90%	EUS: 87–89%
	CEUS: 100%	CEUS: 84.5–89.7%
	FDG-PET: 100%	FDG-PET: 100%
Hepatic invasion, vascular invasion ^{8,15,21}	USG: 67%	USG: NA
	CT: 100%	CT: 100%
	MRI (MRA): 100%	MRI: 100%
Lymph node metastases ⁵⁹	CT: 61.5%	CT: 84.9%
	MRI: 56%	MRI: 89%
Peritoneal metastases ^{60–62}	FDG-PET: 70%	FDG-PET: 97%
	CT: 85–93%	CT: NA
	MRI: 85–90%	MRI: NA
	FDG-PET: 28%	PET: 100%

CEUS: Contrast Enhanced Ultrasound; CT: Computed Tomography; EUS: Endoscopic Ultrasound; FDG-PET: 5-Flouro-deoxyglucose Positron Emission Tomography; GB: Gallbladder; HRUS: High Resolution Ultrasound; MRA: Magnetic Resonance Angiography; MRI: Magnetic Resonance Imaging; NA: Not Available.

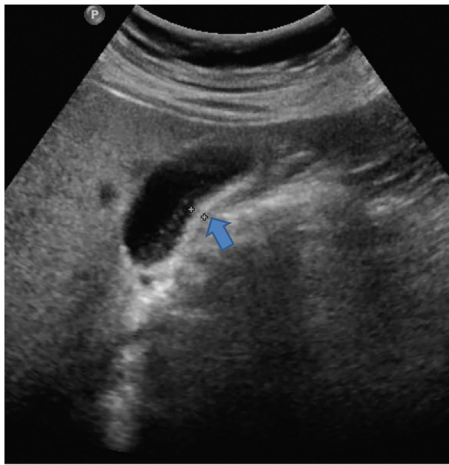


Figure 5 Gray-scale US image shows mild concentric thickening of the GB wall. This appearance is non-specific and is seen in both inflammatory and neoplastic diseases.

study by Inoue et al.²⁶ also reported a limited usefulness of CEUS in diagnosing GBCA. Hirooka et al.²⁷ employed ultrasound contrast agent for EUS and found its discriminatory value in distinguishing GBCA from cholesterol polyp. CE-EUS was also found to be accurate in estimating the depth of tumor invasion. Numata et al. reported high diagnostic rates of CEUS for detection of GBCA (sensitivity, specificity and accuracy of 75%, 100%, and 91% respectively).²⁸ Similarly high diagnostic performance of CEUS was reported by Hattori et al.²⁹ The latter three studies²⁷⁻²⁹ relied on the morphology of the tumor vessels to detect malignancy. The clues to malignancy are arterial branches showing irregularly tortuous extension and tortuous-type tumor vessels. Xie et al.⁴ focussed on destruction of intactness of GB wall on CEUS and reported high sensitivity and specificity of 84.8% and 100% respectively. Unlike Hepatocellular Carcinoma (HCC), a diagnosis of GBCA cannot be based on the finding of arterial hypervascularity

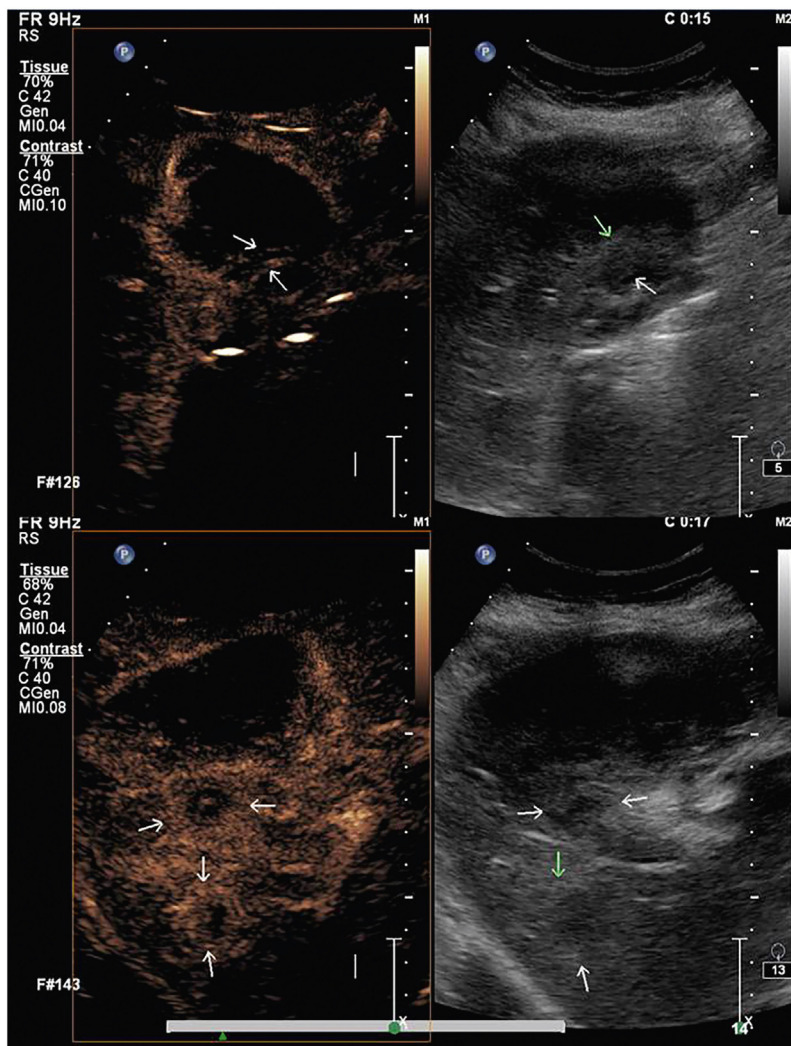


Figure 6 CEUS images of the same patient as in Figure 3 show rapid enhancement (upper panel) and washout pattern (lower panel). Histopathological examination of the resected specimen (following laparoscopic cholecystectomy) revealed malignancy.

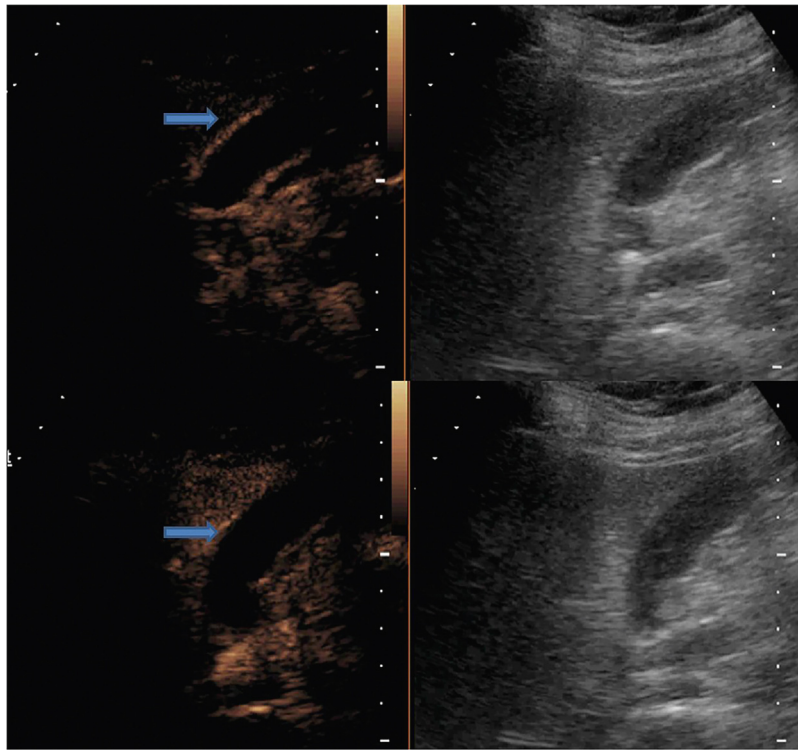


Figure 7 CEUS of two patients show rapid uptake in the GB wall thickening (arrow). Another patient with GBCA, CEUS demonstrates liver metastases as hypo-enhancing lesions (arrows).

and venous phase washout as these contrast dynamics are common to GBCA and benign gallbladder diseases (Figures 5 and 6).^{29,30} Liu et al.⁵ performed a multi-institutional CEUS evaluation of 152 patients with GBCA. They found that CEUS is useful in differentiating GBCA from benign GB diseases. They reported a combination of two findings (destruction of GB wall and linear or branched intraleisional vessels) as indicative of GBCA. Besides, metastatic lesions may be easy to diagnose as they appear relative hypo-enhancing (Figure 7).

EUS

Compared to conventional ultrasound and other cross-sectional imaging techniques, EUS improves the characterization of local disease extent (Figure 8) and involvement of regional lymph nodes in GBCA.

The role of EUS in the accurate diagnosis of the depth of invasion of GBCA has been studied by several investigators.^{6,31} Fujita et al.³¹ classified EUS appearance of GBCA into types based on the depth of invasion and found a good correlation with a histological depth of invasion. Sadamoto et al.⁶ validated the role of EUS in local T-staging of GBCA. Preoperative EUS was performed in 41 patients with GBCA. A diagnostic accuracy of 100%, 75.6%, 85.3%, and 92.7% were reported for pTis, pT1, pT2, and pT3-4 lesions respectively. Jang et al.¹⁹ compared the diagnostic efficacy of HRUS in differential diagnosis and staging compared with that of EUS and MDCT in GB polypoid

lesions and GBCA. In contrast to the previous studies,^{6,31} these authors recorded comparable accuracy of HRUS and EUS even in early GBCA. They attributed this to the technical advances in conventional US.³¹ In a recent study, Imazu et al.³² evaluated 36 patients with GB wall thickening with harmonic contrast enhanced EUS. The authors reported a high sensitivity, specificity and accuracy (89.6%, 98% and 94.4%, respectively) for diagnosis of malignancy.

EUS may also guide needle sampling of GBCA as well as the regional lymph nodes. The application of EUS in this regard has been recently explored. In one of the earliest studies of role of EUS in GBCA by Jhala et al.³³ in 3 patients, malignant cells could be identified in all the patients. Meara et al.³⁴ performed EUS guided Fine Needle Aspiration Cytology (FNAC) in 7 patients with GBCA and reported 100% sensitivity and 80% specificity. They further recorded that a false negative diagnosis may occur in the setting of severe background inflammation. Kim et al.³⁵ performed EUS guided FNAC from GB lesions in 13 patients and from enlarged lymph nodes in 18 patients. They reported a high sensitivity and specificity in diagnosis of both primary as well as the nodal disease. Only one patient suffered acute cholecystitis following FNAC.

MDCT

Considering the current limitations of conventional US and limited experience with CEUS and EUS, MDCT is

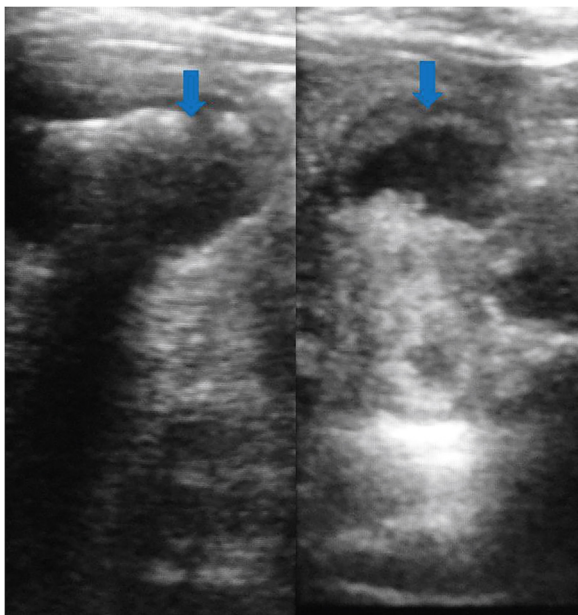


Figure 8 EUS images of GB wall thickening showing resolution of different layers of GB (arrows).

currently the work horse in investigating patients with suspected GBCA. The role of helical CT in GBCA was first described by Yoshimitsu et al.⁷ more than a decade ago. Significant advancement since that time has enhanced the role of CT in patients with GBCA. MDCT allows faster imaging acquisition in multiple phases following intravenous injection of contrast agent and multiplanar reconstructions (Figure 9). Various other post-processing techniques allow an accurate vascular mapping prior to surgery (Figure 10).⁸

Kalra et al.⁸ described the role of dual phase MDCT in staging and determining resectability of GBCA. In this study comprising 20 patients, eight tumors were labeled as resectable and 12 as unresectable. Sensitivity, specificity and diagnostic accuracy of 72.7%, 100%, and 85% respectively were recorded for determining resectability of GBCA. However, this study comprised predominantly

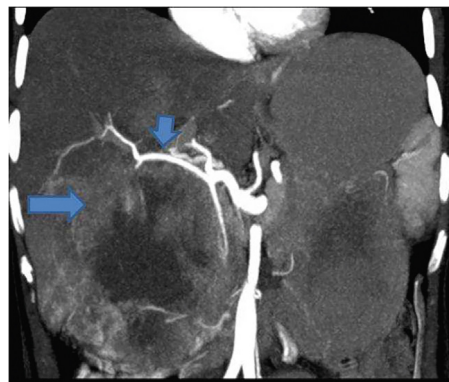


Figure 10 Coronal reformatted MIP image shows a large mass replacing GB fossa (arrow). There is marked displacement of the hepatic artery (short arrow) by the mass.

of relatively advanced stage GBCA. A larger study comprising of 118 patients (68 patients with p-T1 and p-T2 disease), was performed by Kim et al.⁹ to determine the accuracy of MDCT in pre-operative staging of GBCA. These authors reported a high sensitivity, specificity and accuracy in differentiating various T-stages. The overall accuracy was 83.9% for T-staging. Addition of multiplanar reconstructions was found to increase the diagnostic confidence.⁹

Difficulty in distinguishing inflammatory disease from GBCA, particularly early stage GBCA is a well-known limitation of MDCT. Chang et al.³⁶ conducted a study to determine the accuracy of MDCT in distinguishing Xanthogranulomatous Cholecystitis (XGC) from early stage GBCA. They evaluated histopathologically proven cases of T1- and T2-stage GB ($n = 56$) and XGC ($n = 25$) by a pre-operative MDCT. In the GBCA group ($n = 56$), MDCT interpretation was GBCA ($n = 49$), possibility of chronic cholecystitis or GBCA ($n = 3$), possibility of adenomyomatosis or GBCA ($n = 3$) and possibility of XGC or GBCA ($n = 1$). In the XGC group ($n = 25$), 2 cases were falsely labeled as GBCA and differential diagnosis of GBCA was offered in 6 cases on pre-operative MDCT.

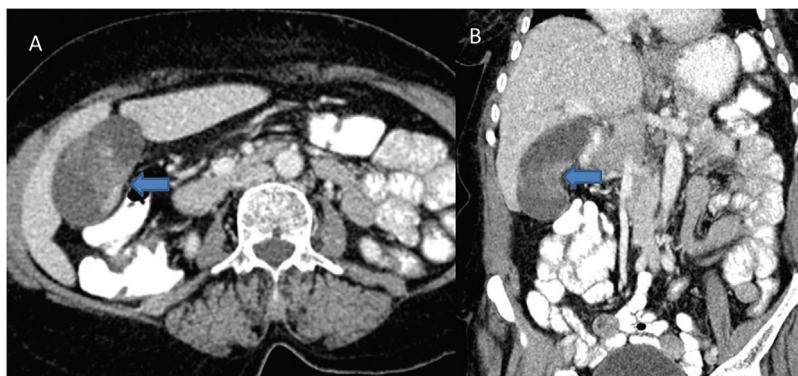


Figure 9 Axial (A) and coronal reformatted (B) images reveal focal asymmetrical thickening of the GB wall (arrows) in the region of body.

Diffuse gallbladder wall thickening, early enhancement of GB wall, continuous mucosal line, hypodense intramural nodule and presence of gallstones were MDCT findings seen more frequently in patients with XGC than patients with GBCA. Lymph node enlargement was the only finding that was noted to be more common in GBCA. Another challenge in imaging GB is the differentiation of GBCA from chronic cholecystitis. In a study by Yun et al., 82 patients including 35 with GBCA and 47 with chronic cholecystitis were evaluated using a biphasic spiral CT.³⁷ Mean wall thicknesses was significantly greater (12.6 mm vs. 6.9 mm) in the GBCA group compared to chronic cholecystitis group. The common enhancement patterns in GBCA were a highly enhanced thick inner wall layer during the arterial phase or a highly enhanced thick inner wall layer during both phases. The most common enhancement pattern of chronic cholecystitis was isoattenuation of the thin inner wall layer during both phases. In another study by Kim et al., enhancement pattern was studied to differentiate benign from malignant GB wall thickening.³⁸ Thicknesses of the inner and outer layers (“thick” enhancing inner layer ≥ 2.6 mm, “thin” outer layer ≤ 3.4 mm), strong enhancement of the inner wall, and irregular contour of the affected wall were found to be significant predictors of malignant GB wall thickening. The two-layer enhancement pattern (strongly enhancing thick inner layer and weakly enhancing or nonenhancing outer layer) and the one-layer enhancement pattern (heterogeneously enhancing thick layer) were significantly associated with GBCA. Adenomyomatosis is a potential mimicker of GBCA on imaging as focal or diffuse thickening of the gallbladder wall is common to both diseases.³⁷ Eida et al.³⁹ evaluated 20 patients with pathologically proven diagnosis of adenomyomatosis or GBCA by a pre-operative MDCT. The authors reported two signs with high accuracy for diagnosis of adenomyomatosis. These included “pearl necklace sign” and uninterrupted mucosal enhancement line. The former

represented GB wall thickening with multiple dilated hypodense intramural Rokitansky–Aschoff sinuses.

Despite these advances, MDCT has low accuracy in detection of peritoneal metastases and lymph node involvement. In the study by Kalra et al.⁸ peritoneal involvement was diagnosed by MDCT only in one patient. However, on surgery, three patients were found to have peritoneal metastases. Similarly, in this study, MDCT could not detect involvement of N1 nodes in 6 patients (8 patients had N1 node involvement on histopathology).

MRI

MRI has a higher soft tissue contrast resolution compared to MDCT. As the imaging appearance of early GBCA is rather non-specific on other imaging modalities, MRI may prove superior. Several researchers have studied the role of MRI in GBCA in evaluating local disease as well as metastases (Figure 11).^{9,40–43} Sagoh et al.⁴⁰ reported the most common MRI pattern of GBCA to be mass forming or diffuse wall thickening. Focal wall thickening with an eccentric mass was reported in three-fourth cases by Schwartz et al.⁴¹ GBCA is typically hypointense on T1W and hyperintense on T2W images. Concurrent gallstones are seen as filling defects and better demonstrated by MRI compared to MDCT.⁹ Following administration of gadolinium chelates, GBCA shows heterogeneous arterial enhancement that persists in the venous phase.⁹ Eaton et al. reported 100% sensitivity and 70% specificity of MRI for detecting malignancy in lesions of 0.8 cm size.⁴²

Attempts have been made to differentiate benign inflammatory diseases from GBCA on MRI. Jung et al.⁴³ reported the MRI findings of acute cholecystitis. The wall thickening in acute inflammation is represented on heavily T2 weighted images (half-Fourier acquisition single shot turbo spin echo) by an ill-defined double-layered pattern with a thickened or interrupted hypointense inner layer (mucosa and muscularis propria) and thick hyperintense outer layer (stroma and serosa). A

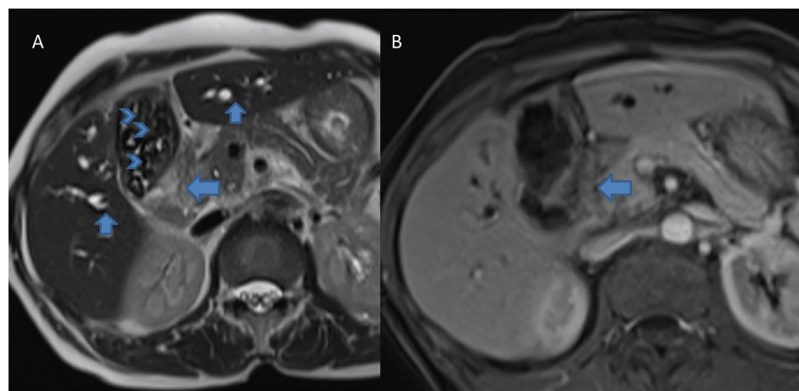


Figure 11 Axial T2 weighted (A) and gadolinium enhanced (B) MR images show soft tissue mass at the neck of the GB (arrows, A and B). Also note bilateral IHBRD (short arrows, A) and cholelithiasis (arrow head, A).

similar pattern is seen in chronic cholecystitis. Wall thickening in chronic cholecystitis may mimic GBCA. High resolution T2W images and arterial phase gadolinium enhanced images may allow differentiation of GBCA from chronic cholecystitis.⁴⁴⁻⁴⁶ There is a relatively smooth and early enhancement of inner layer in chronic cholecystitis compared to irregular enhancement in GBCA.^{44,45} XGC, a specific form of chronic cholecystitis poses a considerable diagnostic challenge. It closely mimics GBCA both clinically and on imaging.⁹ Typical MRI features include GB wall thickening showing areas of isointensity to mild hyperintensity on T2-weighted images. There is slight enhancement at arterial phase and intense enhancement at portal venous of contrast enhancement. Interspersed are necrotic areas or abscesses showing marked hyperintensity on T2-weighted images without contrast enhancement.⁹ However, differentiation of GBCA from XGC even on MRI is a challenge.⁹

Adjacent liver invasion, bile duct invasion, lymph node metastases and vascular invasion are important pre-operative findings that have a profound effect on the surgical planning. Combining MRI with Magnetic Resonance Cholangio-pancreatography (MRCP) (Figure 12) and Magnetic Resonance Angiography (MRA), the radiologist is able to answer all critical questions at pre-operative imaging with variable sensitivity and specificity.⁹ Kim et al.²¹ found 100% sensitivity and around 90% specificity for bile duct and vascular invasion. The sensitivity and specificity were relatively lower for hepatic invasion and lymph node metastasis. However, a subsequent study by Kaza et al.¹³ showed a high sensitivity and specificity for detecting hepatic invasion and lymph node metastases as well. In a recent study on the role of MRI in pre-operative staging of GBCA, Kim et al.⁴⁶ found an overall diagnostic accuracy of 84.9% and 77.9% for T- and N-staging respectively.

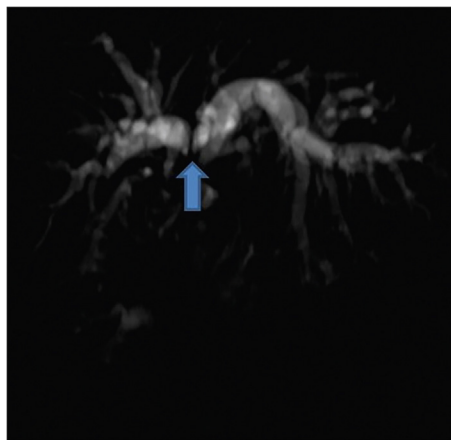


Figure 12 MRCP image in a patient with GBCA shows infiltration and separation of the primary confluence (arrow).

DW-MRI

DW-MRI is a surrogate marker of cellularity.⁴⁷ As GBCA represents a highly cellular lesion, it is expected to show restricted diffusion. Apparent Diffusion Coefficient (ADC) is a quantitative marker of diffusion restriction. Lesions showing restricted diffusion appear dark on ADC maps (Figure 13).⁴⁷

Sugita et al.¹¹ proposed a cut off ADC value ($b = 1000 \text{ s/mm}^2$) of 0.94 for differentiating GBCA from benign diseases. An ADC value of less than 0.94 was found to yield sensitivity and specificity of 83.3% and 100%, respectively in this differentiation. In another study by Irie et al.¹² GBCA was reported to have a high or very high signal on DWI with significantly lower mean ADC than benign lesions. Tan and Lim¹⁰ also reported that GBCA shows hyperintensity on DWI and low signal on ADC maps. However, the authors in this study noted a significant proportion of benign diseases showing similar pattern. Thus, it becomes imperative to interpret DWI findings in the light of basic MRI sequences. DWI has a high sensitivity in detection of liver metastases and lymph node metastases. However, the specificity for nodal metastases is poor.

FDG-PET

FDG-PET has a high sensitivity and specificity in differentiating between benign and malignant diseases compared to conventional US, MDCT and MRI at various sites in the body including head and neck and gastrointestinal tract.⁴⁸⁻⁵⁰ The efficacy of FDG PET in diagnosing GBCA has also been reported.^{51,52} However, most of these studies have reported their results in advanced stage or bulky lesions (Figure 14).^{51,52} The ability to distinguish malignant from benign GB wall thickening is desirable. In this context, only a few studies have been reported.⁵² In a retrospective study by Ai et al.⁵² 12 patients with GB wall thickening identified on US or CT underwent FDG PET to characterize it as benign or malignant. A diagnosis of GBCA was given based on high uptake in four patients. On histopathology, three patients had GBCA while one had chronic cholecystitis. The diagnosis of chronic cholecystitis offered on FDG PET was confirmed in 2 patients who underwent surgery. In rest of the patients, follow up was done. In a recent study by Lee et al.¹⁴ FDG-PET was found to have no significant advantage over MDCT for diagnosis of GBCA. However, a significantly higher positive predictive value (94.1% vs. 77.5%) was recorded for FDG-PET compared to MDCT for detection of regional lymph node metastasis (Figure 15). A significantly higher sensitivity (94.7% vs. 63.2%) was also reported for detection of distant metastases compared to MDCT. Kim et al.⁵³ evaluated the role of FDG-PET in predicting the resectability of GBCA. In their study of 26 patients with GBCA, they found that FDG-PET has a higher accuracy (compared to MDCT) in predicting resectability in

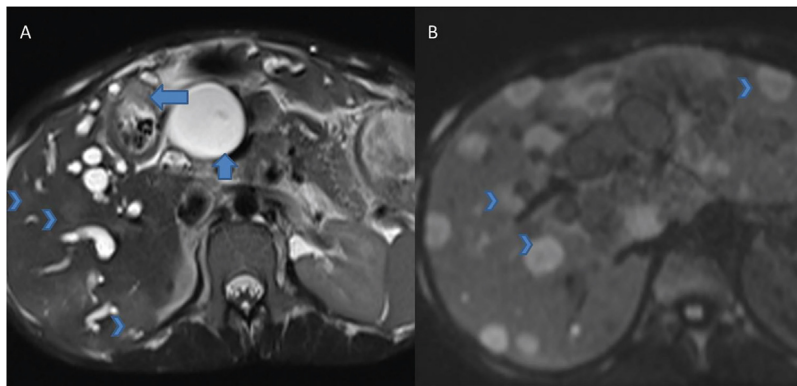


Figure 13 Axial T2 weighted image (A) reveal asymmetrical thickening of the GB wall (arrow, A). Marked dilatation of the CBD (short arrow, A) is due to extrinsic compression by lymph nodes (not shown). Also note subtle hyperintense lesions (arrow heads) and bilateral IHBRD. Diffusion weighted MR (B) shows diffusion restriction (arrow heads) within the focal liver lesions suggestive of metastases.

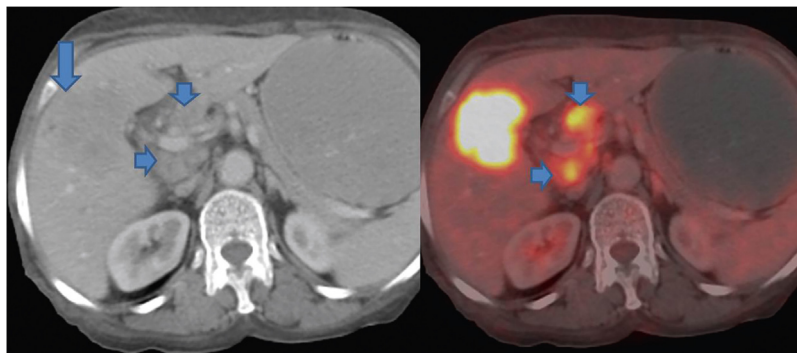


Figure 14 PET-CT shows an ill-defined hypodense mass replacing the GB fossa (arrow) showing marked FDG avidity. In addition, multiple FDG avid periportal lymph nodes are seen (short arrows).

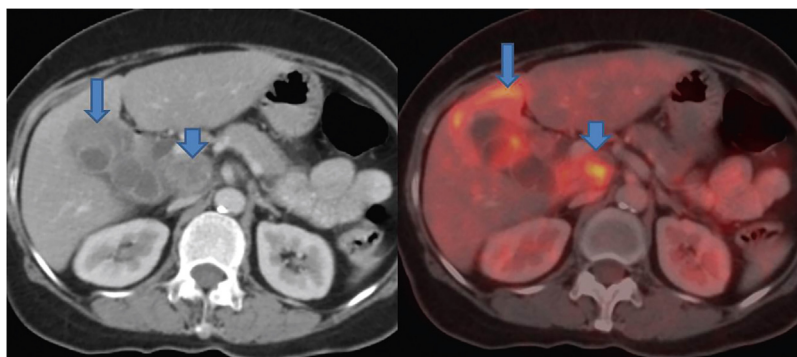


Figure 15 PET-CT shows asymmetrical mural thickening of the GB (arrow). There is adjacent liver infiltration showing FDG avidity (arrow). A large necrotic FDG avid periportal lymph node is also seen (short arrow).

patients who underwent surgical resection. However, there were 3 false negative cases.

IMAGE GUIDED FINE NEEDLE ASPIRATION CYTOLOGY (FNAC)

Several recent studies have established the efficacy of ultrasound guided FNAC. In a study by Yadav et al, a

total of 541 US FNAC were performed for the establishment of diagnosis of CAGB over a period of 24 months.⁵⁴ On cytology, 54 aspirates (9.9%) were labeled unsatisfactory due to insufficient material for diagnosis. The negative cases ($n = 50$) were categorized into two groups: normal epithelial cells and inflammatory. Four hundred thirty-seven cases were positive for malignancy. A false negativity rate of 3.1% and sensitivity of 96.8% was

established. In a study by Barhuiya et al., an adequacy rate of 72% was reported as they performed most of the FNAC in a blind fashion.⁵⁵ In a study by Iqbal et al., 50 US guided FNAC were performed.⁵⁶ Smears showed adenocarcinoma 23, undifferentiated carcinoma in 7, dysplasia and suspicion of malignancy in 5, hemorrhagic background without malignant cells in 12 and inflammatory cells with no malignancy in 3 cases. Results were compared with open/laparoscopic biopsy. A sensitivity, specificity and PPV of 72.91%, 100% and 100% respectively was reported.

In conclusion, imaging plays an important role in preoperative diagnosis and staging of GBCA, allowing an appropriate management.

CONFLICTS OF INTEREST

The authors have none to declare.

REFERENCES

- Roberts KW, Daugherty SF. Primary carcinoma of the gallbladder. *Surg Clin North Am*. 1986;66:743–749.
- Ouchi K, Sugawara T, Ono H, et al. Diagnostic capability and rational resectional surgery for early gallbladder cancer. *Hepato-gastroenterology*. 1999;46:1557–1560.
- Inui K, Yoshino J, Miyoshi H. Diagnosis of gallbladder tumors. *Intern Med*. 2011;50:1133–1136.
- Xie XH, Xu HX, Xie XY, et al. Differential diagnosis between benign and malignant gallbladder diseases with real-time contrast-enhanced ultrasound. *Eur Radiol*. 2010;20:239–248.
- Liu L-N, Xu H-X, Lu M-D, et al. Contrast-enhanced ultrasound in the diagnosis of gallbladder diseases: a multi-center experience. *PLoS ONE*. 2012;10:e48371.
- Sadamoto Y, Kubo H, Harada N, Tanaka M, Eguchi T, Nawata H. Preoperative diagnosis and staging of gallbladder carcinoma by EUS. *Gastrointest Endosc*. 2003;58:536–541.
- Yoshimitsu K, Honda H, Shinozaki K, et al. Helical CT of the local spread of carcinoma of the gallbladder: evaluation according to the TNM system in patients who underwent surgical resection. *AJR Am J Roentgenol*. 2002;179:423–428.
- Kalra N, Sudha S, Gupta R, et al. MDCT in the staging of gallbladder carcinoma. *AJR Am J Roentgenol*. 2006;186:758–762.
- Kim SJ, Lee JM, Lee JY, et al. Accuracy of preoperative T-staging of gallbladder carcinoma using MDCT. *AJR Am J Roentgenol*. 2008;190:74–80.
- Tan CH, Lim KS. MRI of gallbladder carcinoma. *Diagn Interv Radiol*. 2013;19:312–319.
- Sugita R, Yamazaki T, Furuta A, Itoh K, Fujita N, Takahashi S. High b value diffusion-weighted MRI for detecting gallbladder carcinoma: preliminary study and results. *Eur Radiol*. 2009;19:1794–1798.
- Irie H, Kamochi N, Nojiri J, Egashira Y, Sasaguri K, Kudo S. High b value diffusion-weighted MRI in differentiation between benign and malignant polypoid gallbladder lesions. *Acta Radiol*. 2011;52:236–240.
- Kaza RK, Gulati M, Wig JD, Chawla YK. Evaluation of gall bladder carcinoma with dynamic magnetic resonance imaging and magnetic resonance cholangiopancreatography. *Australas Radiol*. 2006;50:212–217.
- Lee SW, Kim HJ, Park JH, et al. Clinical usefulness of 18F-FDG PET-CT for patients with gallbladder cancer and cholangiocarcinoma. *J Gastroenterol*. 2010;45:560–566.
- Bach AM, Loring LA, Hann LE, Illescas FF, Fong Y, Blumgart LH. Gallbladder cancer: can ultrasonography evaluate extent of disease? *J Ultrasound Med*. 1998;17:303–309.
- Tsuchiya Y. Early carcinoma of the gallbladder: macroscopic features and US findings. *Radiology*. 1991;179:171–175.
- Kim JH, Lee JY, Baek JH, et al. High-resolution sonography for distinguishing neoplastic gallbladder polyps and staging gallbladder cancer. *AJR Am J Roentgenol*. 2015;204:W150–W159.
- Lee JS, Kim JH, Kim YJ, et al. Diagnostic accuracy of transabdominal high-resolution US for staging gallbladder cancer and differential diagnosis of neoplastic polyps compared with EUS. *Eur Radiol*. 2017.
- Jang JY, Kim SW, Lee SE, et al. Differential diagnostic and staging accuracies of high resolution ultrasonography, endoscopic ultrasonography, and multidetector computed tomography for gallbladder polypoid lesions and gallbladder cancer. *Ann Surg*. 2009;250:943–949.
- Choi TW, Kim JK, Park SJ, et al. Risk stratification of gallbladder polyps larger than 10 mm using high-resolution ultrasonography and texture analysis. *Eur Radiol*. 2018;28:195–205.
- Kim JH, Kim TK, Eun HW, et al. Preoperative evaluation of gallbladder carcinoma: efficacy of combined use of MR imaging, MR cholangiography, and contrast-enhanced dual-phase three-dimensional MR angiography. *J Magn Reson Imaging*. 2002;16:676–684.
- Lin MX, Xu HX, Lu MD, et al. Diagnostic performance of contrast-enhanced ultrasound for complex cystic focal liver lesions: blinded reader study. *Eur Radiol*. 2009;19:358–369.
- Chen LD, Xu HX, Xie XY, et al. Intrahepatic cholangiocarcinoma and hepatocellular carcinoma: differential diagnosis with contrast-enhanced ultrasound. *Eur Radiol*. 2010;20:743–753.
- Kumagai Y, Kotanagi H, Ishida H, et al. Gallbladder adenoma: report of a case with emphasis on contrast-enhanced US findings. *Abdom Imaging*. 2006;31:449–452.
- Kato T, Tsukamoto Y, Naitoh Y, et al. Ultrasonographic angiography in gallbladder diseases. *Acta Radiol*. 1994;35:606–613.
- Inoue T, Kitano M, Kudo M, et al. Diagnosis of gallbladder diseases by contrast-enhanced phase-inversion harmonic ultrasonography. *Ultrasound Med Biol*. 2007;33:353–361.
- Hirooka Y, Naitoh Y, Goto H, et al. Contrast-enhanced endoscopic ultrasonography in gallbladder diseases. *Gastrointest Endosc*. 1998;48:406–410.
- Numata K, Oka H, Morimoto M, et al. Differential diagnosis of gallbladder diseases with contrast-enhanced harmonic gray scale ultrasonography. *J Ultrasound Med*. 2007;26:763–774.
- Hattori M, Inui K, Yoshino J, et al. Usefulness of contrast-enhanced ultrasonography in the differential diagnosis of polypoid gallbladder lesions. *Nihon Shokakibyō Gakkai Zasshi*. 2007;104:790–798 [in Japanese].
- Claudon M, Cosgrove D, Albrecht T, et al. Guidelines and good clinical practice recommendations for contrast enhanced ultrasound (CEUS)—update 2008. *Ultraschall Med*. 2008;29:28–44.
- Fujita N, Noda Y, Kobayashi G, Kimura K, Yago A. Diagnosis of the depth of invasion of gallbladder carcinoma by EUS. *Gastrointest Endosc*. 1999;50:659–663.
- Imazu H, Mori N, Kanazawa K, et al. Contrast-enhanced harmonic endoscopic ultrasonography in the differential diagnosis of gallbladder wall thickening. *Dig Dis Sci*. 2014 [Epub ahead of print].
- Jhala N, Jhala D, Chhieng DC, et al. Endoscopic ultrasound-guided fine-needle aspiration: a cytopathologist's perspective. *Am J Clin Pathol*. 2003;120:351–367.
- Meara RS, Jhala D, Eloubeidi MA, et al. Endoscopic ultrasound-guided FNA biopsy of bile duct and gallbladder: analysis of 53 cases. *Cytopathology*. 2006;17:42–49.
- Kim HJ, Lee SK, Jang JW, et al. Diagnostic role of endoscopic ultrasonography-guided fine needle aspiration of gallbladder lesions. *Hepatogastroenterology*. 2012;118:1691–1695.

36. Chang BJ, Kim SH, Park HY, et al. Distinguishing xanthogranulomatous cholecystitis from the wall-thickening type of early-stage gallbladder cancer. *Gut Liver*. 2010;4:518–523.
37. Yun EJ, Cho SG, Park S, et al. Gallbladder carcinoma and chronic cholecystitis: differentiation with two-phase spiral CT. *Abdom Imaging*. 2004;29:102–108.
38. Kim SJ, Lee JM, Lee JY, et al. Analysis of enhancement pattern of flat gallbladder wall thickening on MDCT to differentiate gallbladder cancer from cholecystitis. *AJR Am J Roentgenol*. 2008;191:765–771.
39. Eida M, Addelegawad MS, Sirafy-El M. Role of multidetector CT (MDCT) in differentiation between adenomyomatosis and gall bladder cancer. *Egypt J Radiol Nucl Med*. 2012;43:93–97.
40. Sagoh T, Itoh K, Togashi K, et al. Gallbladder carcinoma: evaluation with MR imaging. *Radiology*. 1990;174:131–136.
41. Schwartz LH, Black J, Fong Y, et al. Gallbladder carcinoma: findings at MR imaging with MR cholangiopancreatography. *J Comput Assist Tomogr*. 2002;26:405–410.
42. Eaton JE, Thackeray EW, Lindor KD. Likelihood of malignancy in gallbladder polyps and outcomes following cholecystectomy in primary sclerosing cholangitis. *Am J Gastroenterol*. 2012;107:431–439.
43. Jung SE, Lee JM, Lee K, et al. Gallbladder wall thickening: MR imaging and pathologic correlation with emphasis on layered pattern. *Eur Radiol*. 2005;15:694–701.
44. Demachi H, Matsui O, Hoshihara K, et al. Dynamic MRI using a surface coil in chronic cholecystitis and gallbladder carcinoma: radiologic and histopathologic correlation. *J Comput Assist Tomogr*. 1997;21:643–651.
45. Yoshimitsu K, Honda H, Kaneko K, et al. Dynamic MRI of the gallbladder lesions: differentiation of benign from malignant. *J Magn Reson Imaging*. 1997;7:696–701.
46. Kim SJ, Lee JM, Lee ES, Han JK, Choi BI. Preoperative staging of gallbladder carcinoma using biliary MR imaging. *J Magn Reson Imaging*. 2014 [Epub ahead of print].
47. Le Bihan D, Breton E, Lallemand D, et al. Separation of diffusion and perfusion in intravoxel incoherent motion MR imaging. *Radiology*. 1988;168:497–505.
48. Kitagawa Y, Nishizawa S, Sano K, et al. Prospective comparison of 18F-FDG PET with conventional imaging modalities (MRI, CT, and 67 Ga scintigraphy) in assessment of combined intraarterial chemotherapy and radiotherapy for head and neck carcinoma. *J Nucl Med*. 2003;44:198–206.
49. Kubota K, Yokoyama J, Yamaguchi K, et al. FDG-PET delayed imaging for the detection of head and neck cancer recurrence after radio-chemo-therapy: comparison with MRI/CT. *Eur J Nucl Med Mol Imaging*. 2004;31:590–595.
50. Rodriguez-Fernandez A, Gomez-Rio M, Llamas-Elvira JM, et al. Positron-emission tomography with fluorine-18-fluoro-2-deoxy-D-glucose for gallbladder cancer diagnosis. *Am J Surg*. 2004;188:171–175.
51. Anderson CD, Rice MH, Pinson CW, Chapman WC, Chari RS, Delbeke D. Fluorodeoxyglucose PET imaging in the evaluation of gallbladder carcinoma and cholangiocarcinoma. *J Gastrointest Surg*. 2004;8:90–97.
52. Ai O, Joji K, Torii K, et al. Distinguishing benign from malignant gallbladder wall thickening using FDG-PET. *Ann Nucl Med*. 2006;20:699–703.
53. Kim J, Ryu KJ, Kim C, Paeng JC, Kim YT. Is there any role of positron emission tomography computed tomography for predicting resectability of gallbladder cancer? *J Korean Med Sci*. 2014;29:680–684.
54. Yadav R, Jain D, Mathur SR, Sharma A, Iyer VK. Gallbladder carcinoma: an attempt of WHO classification on fine needle aspiration material. *Cyto J*. 2013;10:12.
55. Barbhuiya. Bhunia S, Kakkar M, Shrivastava B, Tiwari PK, Gupta S. Fine needle aspiration cytology of lesions of liver and gallbladder. *J Cytol*. 2014;31:20–24.
56. Iqbal M, Gondal KM, Qureshi AU, Tayyab M. Comparative study of ultrasound guided fine needle aspiration cytology with open/laparoscopic biopsy for diagnosis of carcinoma gallbladder. *J Coll Physicians Surg Pak*. 2009;19:17–19.
57. Hederström E, Forsberg L. Ultrasonography in carcinoma of the gallbladder. Diagnostic difficulties and pitfalls. *Acta Radiol*. 1987;28(6):715–718.
58. Nishiyama Y, Yamamoto Y, Fukunaga K, et al. Dual-time-point ¹⁸F-FDG PET for the evaluation of gallbladder carcinoma. *J Nucl Med*. 2006;47:633–638.
59. Lee M-J, Yun MJ, Park M-S, et al. Paraaortic lymph node metastasis in patients with intra-abdominal malignancies: CT vs PET. *World J Gastroenterol*. 2009;15(35):4434–4438.
60. Coakley FV, Choi PH, Gougoutas CA, et al. Peritoneal metastases: detection with spiral CT in patients with ovarian cancer. *Radiology*. 2002;223:495–499.
61. Low RN, Barone RM, Lacey C, Sigeti JS, Alzate GD, Sebrechts CP. Peritoneal tumor: MR imaging with dilute oral barium and intravenous gadolinium-containing contrast agents compared with unenhanced MR imaging and CT. *Radiology*. 1997;204:513–520.
62. Leung U, Pandit-Taskar N, Corvera CU, et al. Impact of pre-operative positron emission tomography in gallbladder cancer. *HPB (Oxford)*. 2014;16:1023–1030.